
The statistical thermodynamics of generative diffusion models: Phase transitions, symmetry breaking and critical instability

Luca Ambrogioni^{1,2}

¹Radboud University

²Donders Institute for Brain, Cognition and Behaviour

luca.ambrogioni@donders.ru.nl

Abstract

Generative diffusion models have achieved spectacular performance in many areas of generative modeling. While the fundamental ideas behind these models come from non-equilibrium physics, variational inference and stochastic calculus, in this paper we show that many aspects of these models can be understood using the tools of equilibrium statistical mechanics. Using this reformulation, we show that generative diffusion models undergo second-order phase transitions corresponding to symmetry breaking phenomena. We show that these phase-transitions are always in a mean-field universality class, as they are the result of a self-consistency condition in the generative dynamics. We argue that the critical instability that arises from the phase transitions lies at the heart of their generative capabilities, which are characterized by a set of mean field critical exponents. Furthermore, using the statistical physics of disordered systems, we show that memorization can be understood as a form of critical condensation corresponding to a disordered phase transition. Finally, we show that the dynamic equation of the generative process can be interpreted as a stochastic adiabatic transformation that minimizes the free energy while keeping the system in thermal equilibrium.

1 Introduction

Generative modeling is a sub-field of machine learning concerned with the automatic generation of structured data such as images, videos and written language (Bond-Taylor et al., 2021). Generative diffusion models (Sohl-Dickstein et al., 2015), also known as score-based models, form a class of deep generative models that have demonstrated high performance in image (Ho et al., 2020; Song et al., 2021b), sound (Chen et al., 2020; Kong et al., 2020; Liu et al., 2023) and video generation (Ho et al., 2022; Singer et al., 2022). Diffusion models were first introduced in analogy with the physics of non-equilibrium statistical physics. The fundamental idea is to formalize generation as the probabilistic inverse of a *forward stochastic process* that gradually turns the target distribution $\phi(\mathbf{y})$ into a simple base distribution such as Gaussian white noise (Sohl-Dickstein et al., 2015; Song et al., 2021a). Recently, several works suggested that many of the dynamical properties of generative diffusion models can be understood using concepts such as spontaneous symmetry breaking (Raya and Ambrogioni, 2023; Biroli and Mézard, 2023; Biroli et al., 2024), and phase transitions (Biroli et al., 2024; Sclocchi et al., 2024). These theoretical and experimental results suggest a deep connection between generative diffusion and equilibrium statistical physics. However, these works do not directly use an equilibrium formulation, which makes it difficult to directly translate results and techniques from one field to the other. In this paper using theoretical arguments, we will show that generative diffusion models can be understood and analyzed using the tools of equilibrium statistical physics. Specifically, we define a family of Boltzmann distributions over the noise-free states, which are



Figure 1: Generative process for a digit taken from the MNIST dataset.

interpreted as (unobservable) microstates during the diffusion process. Using this reformulation, we show that generative diffusion models can undergo second-order phase transitions of the mean-field type, corresponding to the generative spontaneous symmetry breaking first discussed in (Raya and Ambrogioni, 2023) and further studied in Biroli et al. (2024); Li and Chen (2024) and in Sclocchi et al. (2024). In our analysis, the time dependent variance plays the role of a temperature parameter. We obtain a self-consistent equation of state for the system, which corresponds to the fixed-point equation of the generative dynamics. We also show that the generative dynamics minimizes a regularized Helmholtz free energy, which connects diffusion models to other energy-based models in the machine learning and theoretical neuroscience literature (Friston, 2010). Finally, similarly to what was done in Lucibello and Mézard (2024) for associative networks, we use the statistical physics of disordered systems to characterize the transition between generalization and memorization as a disordered phase transition. To validate the theoretical predictions, we present an overview of the recent theoretical and experimental literature discussing symmetry breaking phenomena and phase transitions in trained diffusion models.

2 Preliminaries on generative diffusion models

The goal of diffusion modeling is to sample from a potentially very complex target distribution $\phi(\mathbf{y})$, which we model as the initial boundary condition of a (forward) stochastic process that removes structure by injecting white noise. In order to simplify the derivations, here we assume the forward process to be a mathematical Brownian motion. Other forward processes are more commonly used in the applied literature, such as the variance preserving process (e.g. a non-stationary Olsten-Uhlenbeck process) (Song et al., 2021b). However, most of the qualitative thermodynamic properties are shared between these models. The mathematical Brownian motion is defined by the following Langevin equation:

$$\mathbf{x}(t + dt) = \mathbf{x}(t) + \sigma \mathbf{w}(t) \sqrt{dt} \quad (1)$$

where dt is an infinitesimal increment, σ is the instantaneous standard deviation of the stochastic input and $\mathbf{w}(t)$ is a standard Gaussian white noise process. The marginal probabilities defined by Eq. 1 with $\phi(\mathbf{y})$ as initial boundary condition can be expressed analytically as follows:

$$p_t(\mathbf{x}) = \frac{1}{\sqrt{2\pi t\sigma^2}} \mathbb{E}_{\mathbf{y} \sim \phi} \left[e^{-\frac{\|\mathbf{x} - \mathbf{y}\|_2^2}{2t\sigma^2}} \right] \quad (2)$$

where the expectation is taken with respect to the target distribution $\phi(\mathbf{y})$. A generative model can then be obtained by "inverting" Eq. 1. The inverse equation is

$$\mathbf{x}(t - dt) = \mathbf{x}(t) - \sigma^2 \nabla \log p_t(\mathbf{x}) + \sigma \mathbf{w}(t) \sqrt{dt}, \quad (3)$$

which can be shown to give the same marginal distributions in Eq. 2 if the process is initialized with appropriately scaled white-noise (Anderson, 1982). The function $\nabla \log p_t(\mathbf{x})$ is known as the score in the literature. If the score is available for all values of \mathbf{x} and t , we can then sample from $\phi(\mathbf{y})$ by integrating Eq. 3 using numerical methods.

2.1 Training diffusion models as denoising autoencoders

While the score of the target distribution is generally not available analytically, a deep network can be trained to approximate it using a large set of samples (Song et al., 2021a). We refer to the network as a vector valued function $\mathbf{f}(\mathbf{x}(t), t)$. Deep networks are parameterized by a large number of weights and biases. However, since we are not interested in the details of the specific parameterization, here we will report the functional loss:

$$\mathcal{L}[\mathbf{f}(\cdot, \cdot)] = \int_0^{t_{\text{end}}} \mathbb{E}_{\mathbf{y}, \mathbf{x}(t)} \left[\frac{1}{2} \left\| \frac{\mathbf{x}(t) - \mathbf{y}}{\sqrt{t\sigma^2}} - \mathbf{f}(\mathbf{x}(t), t) \right\|_2^2 \right] d\Psi(t), \quad (4)$$

where $\Psi(t)$ is a cumulative distribution with support in $(0, t_{\text{end}})$ and $\mathbf{x}(t)$ is sampled conditional on \mathbf{y} using the propagator of the forward Langevin equation. Note that $\mathbf{x}(t) - \mathbf{y}/\sqrt{t\sigma^2}$ is simply the total noise added up to time t , which implies that the network learns how to predict the noise that corrupted the input data. The score function $\nabla \log p_t(\mathbf{x})$ can then be obtained from the optimized network $\mathbf{f}^* = \text{argmin } \mathcal{L}[f]$ using the following formula (Anderson, 1982):

$$\nabla \log p_t(\mathbf{x}) \approx -(t\sigma^2)^{-1} f^*(\mathbf{x}(t), t). \quad (5)$$

In other words, the score is proportional to the optimal estimate of the noise given the noise-corrupted state. Therefore, once the network is trained to minimize Eq. 4, synthetic samples can be generated by sampling $\mathbf{x}(t_{\text{end}})$ from the boundary noise, computing the score using Eq. 5 and integrating backward Eq. 3 using numerical methods. An example of this generative dynamics for a network trained on natural images is shown in Fig. 1.

3 Diffusion models as systems in equilibrium

As defined above by the forward and inverse Langevin equation, generative diffusion models are non-equilibrium systems. In this section, we shall show that they can be reformulated using the language of equilibrium statistical mechanics, which will allow us to analyze their thermodynamics properties. As we shall see, the generative process can then be derived as an adiabatic transformation that keeps the thermodynamic system in equilibrium.

The starting point for any model in statistical mechanics is the definition of the relevant microstates. In physics, the microstate is considered an unobservable quantity. If we can observe a noise-corrupted data $\mathbf{x}^*(t)$, the obvious unobservable quantity of interest is the noise-free initial state $\mathbf{x}^*(0) = \mathbf{y}^*$. The next step is to define a Hamiltonian function on the set of microstates and all values of the time t . We can do this by considering the conditional probability of the data \mathbf{y} given a noisy state \mathbf{x}_t :

$$p(\mathbf{y} | \mathbf{x}, t) = \frac{1}{p(\mathbf{x}, t)} e^{-\frac{\|\mathbf{x}-\mathbf{y}\|_2^2}{2t\sigma^2} - \log \phi(\mathbf{y})} = \frac{1}{Z(\mathbf{x}, t)} e^{-\mathcal{H}(\mathbf{y}; \mathbf{x}, t)}, \quad (6)$$

which we can interpret as a Boltzmann distribution over the microstates \mathbf{y} with Hamiltonian

$$\mathcal{H}(\mathbf{y}; \mathbf{x}, t) = (t\sigma^2)^{-1} \left(\frac{1}{2} \|\mathbf{y}\|_2^2 - \mathbf{x} \cdot \mathbf{y} \right) - \log \phi(\mathbf{y}) \quad (7)$$

and partition function

$$Z(\mathbf{x}, t) = \int e^{-\mathcal{H}(\mathbf{y}; \mathbf{x}, t)} d\mathbf{y}. \quad (8)$$

The statistical properties of this ensemble are crucial for diffusion models as they determine the score function, which can now be expressed as a Boltzmann average:

$$\nabla \log p_t(\mathbf{x}) = \beta(\langle \mathbf{y} \rangle_{\mathbf{x}} - \mathbf{x}), \quad (9)$$

where

$$\langle \mathbf{y} \rangle_{\mathbf{x}} = \int \mathbf{y} \frac{e^{-\mathcal{H}(\mathbf{y}; \mathbf{x}, t)}}{Z(\mathbf{x}, t)} d\mathbf{y}. \quad (10)$$

Intuitively, this equation tells us that the score vector directs the system towards the posterior average $\langle \mathbf{y} \rangle_{\mathbf{x}}$. This leads to radically different kinds of behaviors depending on the concentration of the Boltzmann weights. As we shall see, studying the thermodynamics determined by these weights will allow us to understand several important qualitative and quantitative features of the generative dynamics. For example, as we will see in later sections, after a condensation phase transition the score will only depend on a small number of data-points, which can be detected by studying the concentration of the weights.

The thermodynamic system defined by Eq. 6 does not have a true temperature parameter. However, the quantity σt plays a very similar role to temperature in classical statistical mechanics. Moreover, in the Hamiltonian given by Eq. 7, the dynamic variable \mathbf{x} is analogous to the external field term in magnetic systems, which can bias the distribution of microstates towards the patterns 'aligned' in its direction. We can imagine \mathbf{x} as being a "slower" thermodynamic variable that interacts (adiabatically) with the statistics of the microstates.

3.1 Example 1: Two deltas

Most of the complexity of the generative dynamics comes from the target distribution $\phi(\mathbf{y})$. However, simple toy models can be used to draw general insights that often generalize to complex target distributions. A simple but informative example is given by the following target

$$\phi(y) = \frac{1}{2} (\delta(y+1) + \delta(y-1)) \quad (11)$$

where y is equal to either -1 or 1 with probability $1/2$. Assuming the binary constraint, this results in the following diffusion Hamilton

$$\mathcal{H}(\mathbf{y}; \mathbf{x}, t) = (t\sigma^2)^{-1} \left(\frac{1}{2}y^2 - xy \right) - \log 2 \quad (12)$$

and the partition function

$$Z(x, t) = e^{\beta/2} \cosh(\beta(t)x) . \quad (13)$$

where $\beta(t) = \sigma^2 t$. Note that this is the same partition function of the Curie-Weiss model of ferromagnetism, which suggests a connection with mean-field theory.

3.2 Example 2: Discrete dataset

In real application, generative diffusion models are trained on a large but finite dataset $D = \{\mathbf{y}_1, \dots, \mathbf{y}_N\}$. Sampling from this dataset correspond to the target distribution

$$\phi(\mathbf{y}) = \frac{1}{N} \sum_{j=1}^N \delta(\mathbf{y} - \mathbf{y}_j) . \quad (14)$$

If the data-points are all normalized so as to have norm equal to one, this results in the partition function

$$Z(\mathbf{x}, t, N) = \frac{e^{-\beta(t)/2}}{N} \sum_{j=1}^N e^{\beta(t) \mathbf{x} \cdot \mathbf{y}_j} . \quad (15)$$

This partition function will play a central role in the random-energy analysis of the model, which can be used to study the finite sample thermodynamics.

3.3 Example 3: Hyper-spherical manifold

Since datasets are always finite, in practice every trained generative diffusion model corresponds to the discrete model outlined in the previous subsection. However, fitting the dataset exactly leads to a model that can only reproduce the memorized training data. Instead, the hope is that the trained network will generalize and interpolate the samples, thereby approximately recovering the true distribution of the sampled data. Very often, this distribution will span a lower-dimensional manifold embedded in the ambient space.

A simple toy model of data defined in a manifold is the hyper-spherical model introduced in ([Raya and Ambrogioni, 2023](#)):

$$Z(\mathbf{x}, t, d) = \frac{e^{-\beta(t)/2}}{V(d-1)} \int_{S(d-1)} e^{-\beta(t) \mathbf{x} \cdot \mathbf{y}} d\mathbf{y} . \quad (16)$$

where $S(d-1)$ denotes a $d-1$ -dimensional hyper-sphere centered at zero with volume $V(d-1)$. The "two delta" model is a special case of this model for an ambient dimension equal to one. As we will see in further section, this data distribution is very tractable in the infinite dimensional (i.e. thermodynamic) limit as it converges to a distribution of normalized Gaussian variables, which removes the quadratic terms in the Hamiltonian.

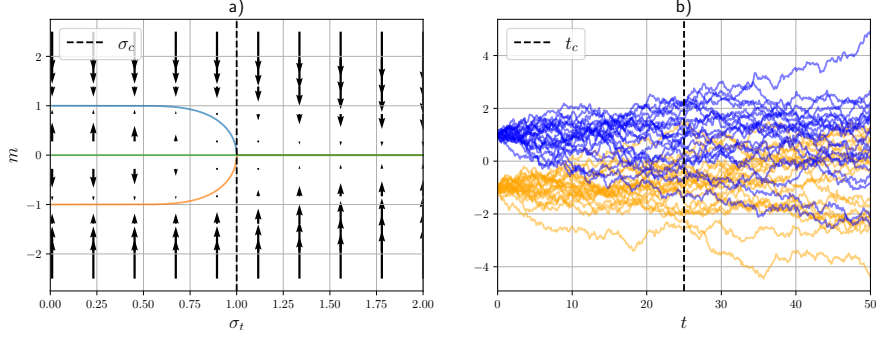


Figure 2: Visualization of a phase transition in a simple diffusion model (two deltas). a) Order parameter paths and (regularized) free energy gradients. The dashed line denotes the critical value of $\sigma_t = \sqrt{t}\sigma_0$. b) Forward process. The dashed line denotes time critical time.

4 Free energy, magnetization and order parameters

Using our interpretation of $\beta(t) = (t\sigma^2)^{-1}$ as the inverse temperature parameter, we can define the Helmholtz free energy as follows

$$\mathcal{F}(\mathbf{x}, t) = -\beta^{-1}(t) \log Z(\mathbf{x}, t). \quad (17)$$

The expected value of the pattern \mathbf{y} given \mathbf{x} can then be expressed the gradient of the free energy with respect to \mathbf{x} :

$$\langle \mathbf{y} \rangle_{\mathbf{x}} = -\nabla \mathcal{F}(\mathbf{x}, t). \quad (18)$$

This formula suggests an analogy between diffusion models and magnetic systems in statistical physics. The noisy state \mathbf{x} can be interpreted as an external magnetic field, which induces the state of "magnetization" $\langle \mathbf{y} \rangle_{\mathbf{x}}$. In this analogy, a diffusion model is magnetized when its distribution is biased towards a sub-set of the possible microstates.

In physics, the 'external field' variable \mathbf{x} is usually assumed to be controlled by the experimenter. On the other hand, in generative diffusion models \mathbf{x} is a dynamic variable that, under the reversed dynamics, is itself attracted towards $\langle \mathbf{y} \rangle_{\mathbf{x}}$ by the drift term:

$$\nabla \log p_t(\mathbf{x}) \propto (\langle \mathbf{y} \rangle_{\mathbf{x}} - \mathbf{x}) \quad (19)$$

In other words, if we ignore the effect of the dispersion term, the state of the system is driven towards self-consistent points where \mathbf{x} is equal to $\langle \mathbf{y} \rangle_{\mathbf{x}}$. It is therefore interesting to study the self-consistency equation

$$\mathbf{m}(\mathbf{h}, t) = -\nabla \mathcal{F}(\mathbf{m}(\mathbf{h}, t) + \mathbf{h}, t), \quad (20)$$

which defines the self-consistent solutions $\mathbf{m}(t)$ where the state is identical to the expected value. In the equation, we introduced a perturbation term \mathbf{h} , which will allow us to study how the systems react to perturbations. For $\mathbf{h} = 0$, the equation can be equivalently re-expressed as the fixed point equation of the reversed drift:

$$\nabla \log p_t(\mathbf{m}(\mathbf{0}, t)) = \mathbf{0}. \quad (21)$$

For $t \rightarrow \infty$, this equation admits the single "trivial" solution $\mathbf{m} = \langle \mathbf{y} \rangle_0$, where $\langle \cdot \rangle_0$ denotes expectation with respect to the target distribution $\phi(\mathbf{y})$. In analogy with magnetic systems, we can interpret $\mathbf{m}(\mathbf{h}, t)$ as an order parameter and this equation as a thermodynamic equation of state. This analogy suggests that $\mathbf{m}(\mathbf{h}, t)$ can be interpreted as a 'spontaneous magnetization' of the system. From this point of view, we can conceptualize the generative process as a form of self-consistent spontaneous symmetry breaking, where the system aligns with one of the many possible target points. In the following sections, we will formalize this insight by characterizing the critical behavior of this system.

Readers familiar with statistical physics will recognize that Eq. 20 is formally identical to the self-consistency conditions used in the mean field approximation, where the external field term in one location is assumed to be determined by the magnetization of all other locations. However, it is important to note that in the case of a diffusion model, this self-consistent coupling is not approximate,

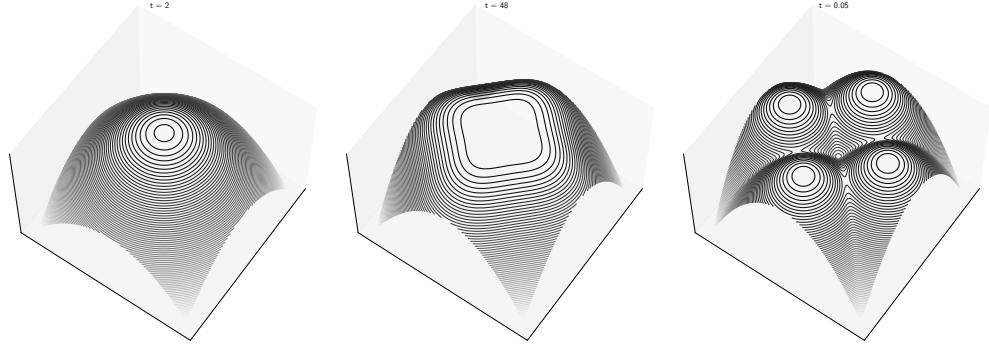


Figure 3: Negative free energy of a "four delta" 2d diffusion model for different values of the time variable. The target points are at $(1, 0)$, $(0, 1)$, $(-1, 0)$ and $(0, -1)$.

as it is a natural consequence of the dynamics. Nevertheless, the formal analogy implies that the thermodynamics of generative diffusion models is formally identical to the thermodynamics of mean field models.

4.1 The susceptibility matrix

In the physics of magnetic systems, the magnetic susceptibility matrix determines how much the different magnetization components are sensitive to the components of the external magnetic field. Similarly, in diffusion models we can define a susceptibility matrix:

$$\chi_{ij}(t) = \left. \frac{\partial m_i}{\partial h_j} \right|_{\mathbf{h}=0}, \quad (22)$$

which tells us how sensitive the expected value is to changes in the noisy-state $\mathbf{x}(t)$. The susceptibility matrix has a great value in interpreting the dynamics of the generative denoising process, as it informs us on how random fluctuations in each component of the state $\mathbf{x}(t)$ are propagated to the other components. For example, in the context of image generation, a random fluctuation of "green" at the bottom of an image will propagate to the rest, originating the image of a forest.

4.2 The regularized free energy

So far, we characterized the thermodynamic state of diffusion model at time t by its Boltzmann distribution. The dynamics of the system can now be recovered as a form of (stochastic) free energy minimization:

$$\mathbf{x}(t - dt) = \mathbf{x}(t) - \beta(t) \nabla \tilde{\mathcal{F}}(\mathbf{x}, t) dt + \sigma \mathbf{w}(t) \sqrt{dt}, \quad (23)$$

where $\tilde{\mathcal{F}}$ is the free-energy plus a L_2 regularization term:

$$\tilde{\mathcal{F}}(\mathbf{x}, t) = \mathcal{F}(\mathbf{x}, t) + \frac{1}{2} \|\mathbf{x}\|_2^2 \quad (24)$$

This can be seen as a form of adiabatic approximation, where the dynamics of the 'slow' variable \mathbf{x} is obtained by assuming that the system is maintained in thermal equilibrium along the diffusion trajectory. The symmetry breaking can now be detected as a change of shape in the regularized free energy, which transitions from a convex shape with a single global minimum to a more complex shape with potentially several meta-stable points (see Fig. 3). The reformulation of the dynamics in term of the gradient of a free energy allows us to interpret generative diffusion models as a kind of energy-based machine learning models (LeCun et al., 2006), as discussed in (Hoover et al., 2023) and (Ambrogioni, 2023). The main difference is that the (free) energy is not learned directly but it is instead implicit in the learned score function. The connection suggests potential connection with the free energy principle in theoretical neuroscience, which is used to characterize the stochastic dynamics of biological neural systems (Friston, 2010).

5 Connecting the thermodynamics of diffusion models and physical systems: The diffused Ising model

While most of the formulas presented in this manuscript have a very close analogy with formulas in statistical physics, there are some subtle interpretative differences that could create confusion in the reader. To clarify these issues, we will discuss the *diffused Ising model*, which will provide a bridge between the two views. Consider a diffusion model with a target distribution supported on d -dimensional vectors \mathbf{y} with entries in the set $\{-1, 1\}$. The log-probability of the target distribution is defined by the following formula:

$$\log \phi(\mathbf{y}) = -\frac{1}{2T} \sum_{j \neq k} y_j y_k W_{jk} + c, \quad (25)$$

where \mathbf{W} is a symmetric coupling matrix, T is a temperature parameter and c is a constant. Up to constants, this is of course the log-probability of an Ising model without the external field term. From Eq. 7, up to constant terms, we obtain the following Hamiltonian for the diffusion model:

$$\mathcal{H}(\mathbf{y}; \mathbf{x}, t, T) = -\beta(t) \mathbf{x} \cdot \mathbf{y} + \frac{1}{2T} \sum_{j \neq k} y_j y_k W_{jk}, \quad (26)$$

which is almost identical to the Hamiltonian of an Ising model coupled to a location-dependent external field \mathbf{x} . Nevertheless, the quantity $\beta(t) = (t\sigma^2)^{-1}$, which we loosely interpreted as a "inverse temperature", does not divide the coupling part of the Hamiltonian, which results in a radically different behavior. In fact, $t\sigma^2$ only modulates the susceptibility to the field term and it therefore does not radically alter the phase of the model, which depends on the Ising temperature parameter T . Instead, the interesting phase transition of the diffusion models is a consequence of the self-consistency relation in Eq. 20, which characterizes the branching of the fixed-points of the generative stochastic dynamics. From the point of view of statistical physics, Eq. 20 can be seen as the result of a mean-field approximation, where the average magnetization is coupled to the external field. However, it is important to keep in mind that, in a diffusion model, this mean-field approach does not represent the coupling between individual sites, which, as Eq. 26 shows, are instead statistically coupled by the interaction terms in the Hamiltonian. Instead, it can be seen as an idealized mean-field interaction between infinitely many copies of the whole system. In general, the value of T will change the properties of the diffusion model, as the system transitions from its low temperature to its high temperature phase. The dependency of the diffusion dynamics on this transition have been studied in Biroli and Mézard (2023).

6 Phase transitions and symmetry breaking

A spontaneous symmetry breaking happens when this trivial solution for the order parameter branches into multiple solutions at some critical time of t_c . This corresponds to the onset of multi-modality in the regularized free energy $\tilde{\mathcal{F}}(\mathbf{x}, t)$, as visualized in Fig. 3 for a "four deltas" model. In thermodynamic systems, the symmetry breaking corresponds to a (second order) phase transition, which in this case can be detected by the divergence of several state variables around the critical point.

The presence of one (or multiple) phase transitions in diffusion models depends on the target distribution $\phi(\mathbf{y})$. The simplest example is given by the "two deltas", which corresponds to the process visualized in Fig. 2 a. Using this distribution, we obtain the self-consistency equation

$$m = \tanh\left(\frac{m}{t\sigma^2}\right) \quad (27)$$

The solutions of this equation are shown in Fig. 2 b, together with the gradient of the regularized free energy, where we can see the branching of the solutions and the singular behavior around a critical point. Eq. 27 is identical to the mean-field self-consistency equation of an Ising model, from which we can deduce that the critical scaling of this simple generative diffusion models shares its universality class. For example, by Taylor expansion of Eq. 27 around $t_c = 1$, we see that

$$m \sim (-\tau)^{1/2} \quad (28)$$

with $\tau = t - t_c$, which is valid for t smaller than t_c .

6.1 Generation and critical instability

As shown in (Raya and Ambrogioni, 2023), spontaneous symmetry breaking phenomena play a central role in the generative dynamics of diffusion models. Consider the simple "two deltas" model. For $t \gg t_c$, the dynamics is mean-reverting towards a unique fixed-point $\mathbf{m}(\mathbf{0}, t)$. Around $t = t_c$, the order parameter splits into three "branches", an unstable one corresponding to the mean of the target distribution and two stable ones corresponding to the two target points. Importantly, at the critical point the susceptibility defined in Eq. 22 diverges, implying that the system becomes extremely reactive to fluctuations in the noise. This instability is determined by the critical exponents δ and γ and , defined by the relations

$$h_j \propto m_j^{\delta_j}, \quad (29)$$

and

$$\chi_{ij} \propto (-\tau)^{\gamma_{ij}}. \quad (30)$$

Note that, in the general case the critical exponents can be different for different coordinates and matrix entries. These divergences give rise to something we refer to as *critical generative instability*. We conjecture that the diversity of the generated samples crucially depends on a proper sampling of this critical region.

7 Associative memory and Hopfield networks

Associative memory networks are energy-based learning systems that can store patterns (i.e. memories) as meta-stable states of a parameterized energy function (Hopfield, 1982; Abu-Mostafa and Jacques, 1985; Krotov, 2023). There is a substantial body of literature on the thermodynamic properties of associative memory networks (Strandburg et al., 1992; Volk, 1998; Marullo and Agliari, 2020). The original associative memory networks, also known as *Hopfield networks*, are defined by the energy function $E(\mathbf{x}) = \frac{1}{2} \mathbf{x}^T \mathbf{W} \mathbf{x}$ under the constraints of binary entries for the state vector. In a Hopfield network, a finite number of training patterns \mathbf{y}_j are encoded into a weight matrix $\mathbf{W} = \sum_j \mathbf{y}_j \mathbf{y}_j^T$, which usually gives the correct minima when the number of patterns is on the order of the dimensionality. Associative memory networks can reach much higher capacity by using exponential energy function (Krotov and Hopfield, 2016; Demircigil et al., 2017; Krotov, 2023). For example, (Ramsauer et al., 2021) introduces the use of the following function

$$E(\mathbf{x}) = -\beta^{-1} \log \left(\sum_j e^{\beta \mathbf{x} \cdot \mathbf{y}_j} \right) + \frac{1}{2} \|\mathbf{x}\|_2^2, \quad (31)$$

which can be proven to provide exponential scaling of the capacity and it is related to the transformers architectures used in large language models (Ramsauer et al., 2021). By inspection of Eq. 31, we can see that this energy function is equivalent to the regularized Helmholtz free energy of a diffusion models trained on a mixture of delta distributions (Ambrogioni, 2023):

$$\phi(\mathbf{y}) = \sum_j \delta(\mathbf{y} - \mathbf{y}_j), \quad (32)$$

which gives a free energy with the same fixed-point structure of Eq. 31 at the zero temperature limit. Note that, while the dynamics of a diffusion model does not necessarily act as an optimizer in the general case, the free energy is exactly optimized when $\phi(\mathbf{y})$ is a sum of delta functions, making the dynamics of the model exactly equivalent to the optimization of Eq. 31 for $\beta \rightarrow \infty$. Given this connection, most of the results presented in this paper can be re-stated for associative memory networks. However, generative diffusion models are more general as they can target arbitrary mixtures of continuous and singular distributions. As we shall see in the next section, the modern Hopfield Hamiltonian plays a crucial role in studying finite sample effects such as data memorization (Lucibello and Mézard, 2024).

8 The random energy thermodynamic of diffusion models on sampled datasets

As we saw in the previous sections, using the target density $\phi(\mathbf{y})$, we can define an Hamiltonian function, and consequently equilibrium thermodynamic system, that captures the statistical properties

of the corresponding generative diffusion dynamics. From the point of view of machine learning, this corresponds to a denoising network perfectly trained on an infinitely large dataset. Consequently, this analysis misses some important properties that arise when the models are trained on finite datasets sampled independently from $\phi(\mathbf{y})$. In particular, the exact model cannot capture the phenomenon of memorization (overfitting), where the model fails to generalize beyond its training set.

We can analyze this regime using the statistical physics of disordered systems, where the quenched partition function depends on N randomly sampled training points:

$$Z_N(\mathbf{x}, \beta(t)) = \frac{1}{N} \sum_{j=1}^N e^{-\beta(t) \left(\frac{1}{2} \|\mathbf{y}_j\|_2^2 + \mathbf{x} \cdot \mathbf{y}_j \right)}, \quad (33)$$

where $\mathbf{y}_j \sim \phi(\mathbf{y})$. The idea is that we can understand the finite sample properties of diffusion models by studying how the partition function and other thermodynamic quantities fluctuate as a function of the random sampling. This is analogous to the physics of glasses, where the thermodynamic properties depend randomly on the (disordered) structure of a piece of material. By defining $E_j(\mathbf{x}) = \frac{1}{2} \|\mathbf{y}_j\|_2^2 - \mathbf{x} \cdot \mathbf{y}_j$, we can re-write this quenched partition function as a random energy model (REM):

$$Z_N(\mathbf{x}, \beta(t)) = \frac{1}{N} \sum_{j=1}^N e^{-\beta(t) E_j(\mathbf{x})}. \quad (34)$$

where the distribution of the energy levels $E_j(\mathbf{x})$ depends on the "external field" \mathbf{x} . The thermodynamic of this model is well known for simple distributions over the energy, and can be studied in more complex cases using the replica method (Mézard et al., 1987).

8.1 Memorization as 'condensation'

The random-energy analysis of a diffusion model is very useful to study the memorization phenomenon, where the diffusion trajectories collapse on the individual sampled datapoints instead of spreading to the underlying target distribution. In machine learning jargon, this phenomenon is known as overfitting. It is clear that a model perfectly trained on a finite dataset (i.e. a model that perfectly reproduces the empirical score) fully memorizes the data without any generalization for $t \rightarrow 0$. However, these over-fitted models can still exhibit generalization for finite values of t since the noise level can be too high to distinguish the individual training points. It was recently discovered that, in the thermodynamic limit, generalization and memorization are demarcated by a disordered symmetry breaking (Lucibello and Mézard, 2024; Biroli et al., 2024). This is a so-called condensation phenomenon, where the probability measures transition from being spread out over an exponential number of configurations to being concentrated on a random small (sub-exponential) set. During condensation, the score is determined by a relatively small number of non-vanishing Boltzmann weight, which eventually direct the dynamics towards one of the training points.

From our theoretical framework, we can find this 'critical time' t_c by studying the random partition function given in Eq. 34 in the thermodynamic limit. This can be done by evaluating the 'participation ration'

$$Y_N(\mathbf{x}, t) = \frac{Z_N(\mathbf{x}, 2\beta(t))}{(Z_N(\mathbf{x}, \beta(t)))^2}, \quad (35)$$

where $1/Y_N(\mathbf{x}, t)$ gives a rough count of the number of configurations with non-vanishing probability. In the REM theory, the participation ration can be used to detect a condensation phase transition, as in this case its value becomes identically equal to zero for $\beta > \beta_c$ in a non-analytic manner.

Consider the simple case where we sampled $N = 2^M$ the data-points from the distribution $\phi(\mathbf{y})$, which is uniform over a d -dimensional hyper-sphere with radius $r = \nu \sqrt{M/2d}$, where ν is a parameter that regulates the standard deviation of the data. In this case, up to an irrelevant constant shift, the random energy becomes

$$E_j(\mathbf{x}) = -\mathbf{x} \cdot \mathbf{y}_j. \quad (36)$$

For high values of d , the distribution of $\mathbf{x} \cdot \mathbf{y}_j$ is approximately a centered Gaussian with variance $\|\mathbf{x}\|_2^2 \nu^2 M/2$ and, which $\phi(\mathbf{y})$ is spherically symmetric, it does not depend on the direction of \mathbf{x} . We

can therefore re-write the expression as a standard REM model:

$$Z_N(\mathbf{x}, \beta(t)) = \frac{1}{2^M} \sum_{j=1}^{2^M} e^{-\tilde{\beta} \tilde{E}_j}. \quad (37)$$

where $\tilde{E}_j \sim \mathcal{N}(0, M/2)$ and $\tilde{\beta} = \nu \beta(t) \|\mathbf{x}\|_2$. For this model, we know that the critical condensation temperature is at $\beta_c = 2\sqrt{\log 2}$ (see Mézard et al. (1987)), which leads to the critical time

$$t_c(\mathbf{x}) = \frac{\nu \|\mathbf{x}\|_2}{2\sigma^2 \sqrt{\log 2}}. \quad (38)$$

This formula was first derived in Lucibello and Mézard (2024) for associative memory models. It can be shown that, at the limit $M \rightarrow \infty$, the expected participation ratio is

$$\mathbb{E}[Y(\mathbf{x}, t)] = \begin{cases} 0, & \text{if } \beta(t) \leq \beta_c \\ 1 - \frac{\beta_c}{\beta(t)}, & \text{if } \beta(t) > \beta_c \end{cases}. \quad (39)$$

This allows us to estimate the number of data-points with non-negligible weight in the score as $n(\mathbf{x}) \approx 1/Y(\mathbf{x}, t)$. Note that t_c does not predict the collapse on an individual data-point, as that would require $Y(\mathbf{x}, t) \approx 1$, which happens at an earlier time. However, it identifies a critical transition in the score function $\nabla \log p(\mathbf{x})$ that demarcates the beginning of a memorization phase. In this phase, the system undergoes further symmetry breaking phase transitions, which break the symmetry between the data-points with non-vanishing weights. The critical behavior of these transitions is analogous to the "two deltas" model.

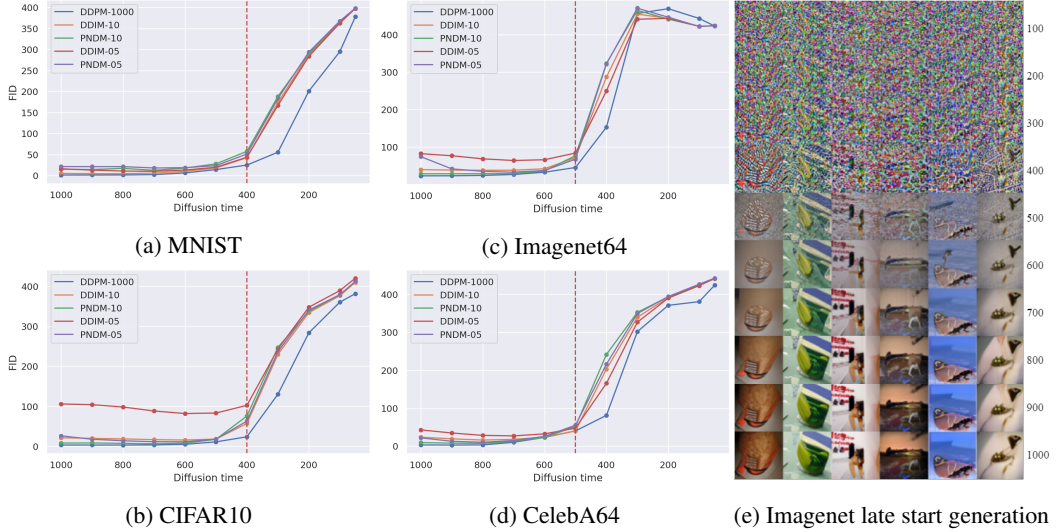


Figure 4: Figure taken from (Raya and Ambrogioni, 2023). Analysis of the model’s performance, as measured by FID scores, for different starting times using three different sampling methods: the normal DDPM sampler with decreasing time steps from $T = 1000$ to 0, and fast sampler DDIM and PNDM for 10 and 5 denoising steps. The vertical line corresponds to the maximum of the second derivative of the FID curve, which offers a rough estimate of the first bifurcation time. (e) Illustrates samples generation on Imagenet64, while progressively varying the starting time from 1000 to 100.

9 Experimental evidence of phase transitions in trained diffusion models

The presence of one or more phase transitions in generative diffusion models is hard to prove theoretically for complex data distributions. However, symmetry breaking can be inferred experimentally from trained networks. For example, Raya and Ambrogioni (2023) showed that the generative performance of models trained on images stay largely invariant when the reversed dynamics is initialized before t_{end} up to a critical point (see Fig. 4e), as far as the system is initialized with a Gaussian with

properly chosen mean vector and covariance matrix. This is consistent with our theoretical analysis since, prior to the first phase transition, the marginal distributions have a single global mode and are well approximated by normal distributions. The effect of this form of symmetry breaking was further studied both experimentally and theoretically in [Sclocchi et al. \(2024\)](#), where it was found that the generative diffusion models trained on natural images undergo a series of phase transitions corresponding to hierarchical class separations, where low-level visual features emerge at earlier times of the diffusion process while higher level semantic features emerge later. These results were further studied in [Biroli et al. \(2024\)](#), where the authors provided a series of analytic formulas for the critical times and verified the prediction experimentally on several image datasets. In particular, it was found that symmetry breaking time corresponding to splits in different classes (e.g. images of dogs and cats) can be predicted based on the eigenvectors of the covariance matrix of the data. Together, these results strongly suggest that generative diffusion models undergo symmetry breaking phase transitions under most realistic data distributions.

10 Conclusions

In this paper, we presented a formulation of generative diffusion models in terms of equilibrium statistical mechanics. This allowed us to study the critical behavior of these generative models during second-order phase transitions and the disordered thermodynamics of models trained on finite datasets. Our analysis establishes a deep connection between generative modeling and statistical physics, which may in the future allow physicists to study these machine learning models using the tools of computational and theoretical physics.

References

Abu-Mostafa, Y. and Jacques, J. S. (1985). Information capacity of the hopfield model. *IEEE Transactions on Information Theory*, 31(4):461–464.

Ambrogioni, L. (2023). In search of dispersed memories: Generative diffusion models are associative memory networks. *arXiv preprint arXiv:2309.17290*.

Anderson, B. D. (1982). Reverse-time diffusion equation models. *Stochastic Processes and their Applications*, 12(3):313–326.

Biroli, G., Bonnaire, T., de Bortoli, V., and Mézard, M. (2024). Dynamical regimes of diffusion models. *arXiv preprint arXiv:2402.18491*.

Biroli, G. and Mézard, M. (2023). Generative diffusion in very large dimensions. *arXiv preprint arXiv:2306.03518*.

Bond-Taylor, S., Leach, A., Long, Y., and Willcocks, C. G. (2021). Deep generative modelling: A comparative review of vaes, gans, normalizing flows, energy-based and autoregressive models. *IEEE transactions on pattern analysis and machine intelligence*.

Chen, N., Zhang, Y., Zen, H., Weiss, R. J., Norouzi, M., and Chan, W. (2020). Wavegrad: Estimating gradients for waveform generation. *arXiv preprint arXiv:2009.00713*.

Demircigil, M., Heusel, J., Löwe, M., Upgang, S., and Vermet, F. (2017). On a model of associative memory with huge storage capacity. *Journal of Statistical Physics*, 168:288–299.

Friston, K. (2010). The free-energy principle: a unified brain theory? *Nature Reviews Neuroscience*, 11(2):127–138.

Ho, J., Jain, A., and Abbeel, P. (2020). Denoising diffusion probabilistic models. *Advances in Neural Information Processing Systems*.

Ho, J., Salimans, T., Gritsenko, A., Chan, W., Norouzi, M., and Fleet, D. J. (2022). Video diffusion models. *arXiv preprint arXiv:2204.03458*.

Hoover, B., Strobel, H., Krotov, D., Hoffman, J., Kira, Z., and Chau, H. (2023). Memory in plain sight: A survey of the uncanny resemblances between diffusion models and associative memories. *arXiv preprint arXiv:2309.16750*.

Hopfield, J. J. (1982). Neural networks and physical systems with emergent collective computational abilities. *Proceedings of the National Academy of Sciences*, 79(8):2554–2558.

Kong, Z., Ping, W., Huang, J., Zhao, K., and Catanzaro, B. (2020). Diffwave: A versatile diffusion model for audio synthesis. *arXiv preprint arXiv:2009.09761*.

Krotov, D. (2023). A new frontier for hopfield networks. *Nature Reviews Physics*, pages 1–2.

Krotov, D. and Hopfield, J. J. (2016). Dense associative memory for pattern recognition. *Advances in Neural Information Processing Systems*.

LeCun, Y., Chopra, S., Hadsell, R., Ranzato, M., and Huang, F. (2006). A tutorial on energy-based learning. *Predicting structured data*, 1(0).

Li, M. and Chen, S. (2024). Critical windows: non-asymptotic theory for feature emergence in diffusion models. *arXiv preprint arXiv:2403.01633*.

Liu, H., Chen, Z., Yuan, Y., Mei, X., Liu, X., Mandic, D., Wang, W., and Plumbley, M. D. (2023). Audiodlm: Text-to-audio generation with latent diffusion models. *arXiv preprint arXiv:2301.12503*.

Lucibello, C. and Mézard, M. (2024). Exponential capacity of dense associative memories. *Physical Review Letters*, 132(7):077301.

Marullo, C. and Agliari, E. (2020). Boltzmann machines as generalized hopfield networks: a review of recent results and outlooks. *Entropy*, 23(1):34.

Mézard, M., Parisi, G., and Virasoro, M. A. (1987). *Spin glass theory and beyond: An Introduction to the Replica Method and Its Applications*, volume 9. World Scientific Publishing Company.

Ramsauer, H., Schäfl, B., Lehner, J., Seidl, P., Widrich, M., Adler, T., Gruber, L., Holzleitner, M., Pavlović, M., Sandve, G. K., et al. (2021). Hopfield networks is all you need. *International Conference on Learning Representations*.

Raya, G. and Ambrogioni, L. (2023). Spontaneous symmetry breaking in generative diffusion models. *Neural Information Processing Systems*.

Sclocchi, A., Favero, A., and Wyart, M. (2024). A phase transition in diffusion models reveals the hierarchical nature of data. *arXiv preprint arXiv:2402.16991*.

Singer, U., Polyak, A., Hayes, T., Yin, X., An, J., Zhang, S., Hu, Q., Yang, H., Ashual, O., Gafni, O., et al. (2022). Make-a-video: Text-to-video generation without text-video data. *arXiv preprint arXiv:2209.14792*.

Sohl-Dickstein, J., Weiss, E., Maheswaranathan, N., and Ganguli, S. (2015). Deep unsupervised learning using nonequilibrium thermodynamics. *International Conference on Machine Learning*.

Song, J., Meng, C., and Ermon, S. (2021a). Denoising diffusion implicit models. *International Conference on Learning Representations*.

Song, Y., Sohl-Dickstein, J., Kingma, D. P., Kumar, A., Ermon, S., and Poole, B. (2021b). Score-based generative modeling through stochastic differential equations. In *International Conference on Learning Representations*.

Strandburg, K. J., Peshkin, M. A., Boyd, D. F., Chambers, C., and O’Keefe, B. (1992). Phase transitions in dilute, locally connected neural networks. *Physical Review A*, 45(8):6135.

Volk, D. (1998). On the phase transition of hopfield networks—another monte carlo study. *International Journal of Modern Physics C*, 9(05):693–700.